Piezomagnetoelectric Effect of Spin Origin in Dysprosium Orthoferrite

Taro Nakajima,[1,*] Yusuke Tokunaga,[1,2] Yasujiro Taguchi,[1] Yoshinori Tokura,[1,3] and Taka-hisa Arima[1,2]
[1]RIKEN Center for Emergent Matter Science (CEMS), Saitama 351-0198, Japan
[2]Department of Advanced Materials Science, University of Tokyo, Kashiwa 277-8561, Japan
[3]Department of Applied Physics and Quantum-Phase Electronics Center (QPEC), University of Tokyo, Tokyo 113-8656, Japan
(Received 16 June 2015; published 5 November 2015)

The piezomagnetoelectric effect, namely, the simultaneous induction of both the ferromagnetic moment and electric polarization by an application of uniaxial stress, was demonstrated in the nonferroelectric antiferromagnetic ground state of $DyFeO_3$. The induced electric polarization and ferromagnetic moment are coupled with each other, and monotonically increase with increasing uniaxial stress. The present work provides a new guiding principle for designing multiferroics where its magnetic symmetry is broken by external uniaxial stress.

DOI: 10.1103/PhysRevLett.115.197205 PACS numbers: 75.85.+t, 62.50.-p

The discovery of spin-driven ferroelectricity in $TbMnO_3$ [1] has opened the door to new frontiers in multiferroics, in which different kinds of ferroic orders coexist [2–4]. The extensive studies on recently explored multiferroics, such as orthorhombic $RMnO_3$ (R is a rare-earth element) [1,5,6], $Ni_3V_2O_8$ [7], $MnWO_4$ [8], etc., demonstrated that ferroelectricity can arise from inversion symmetry breaking cause by magnetic orders. As for the microscopic mechanisms to explain the spin-driven ferroelectricity, the most robust scheme is the inverse Dzyaloshinskii-Moriya (IDM) mechanism [9]; the magnetically induced electric polarization (P) is described as $P \propto e_{i,j} \times (S_i \times S_j)$ [10,11], where $e_{i,j}$ is a unit vector connecting between two spins, S_i and S_j. This formula predicts ferroelectricity in a "cycloidal" spin order, in which the spontaneous electric polarization appears along the twofold axis perpendicular to both the propagation wave vector and $(S_i \times S_j)$, regardless of the symmetry of the underlying chemical lattice.

On the other hand, there are two other mechanisms for the spin-driven ferroelectricity [12–15], namely, the spin-dependent p-d hybridization model [13] and the magnetostriction model [14,15]. In these models, the emergence of ferroelectricity cannot be explained by local spin arrangement alone, but by also taking into account the symmetry of the crystal structure. This suggests in turn that in the *non*-IDM type spin-driven multiferroics, the ferroelectricity can be controlled via changes in crystal structural symmetry.

One of the most primitive ways to control the symmetry of the crystal structure is an application of anisotropic stress. It has recently been demonstrated that an application of compressive uniaxial stress can induce spin-driven electric polarization in $Ba_2CoGe_2O_7$ [16], the origin of whose ferroelectricity is explained by the p-d hybridization model [17]. However, this system originally has a noncentrosymmetric (but nonpolar) crystal structure belonging to the space group of $P\bar{4}2_1m$, in which the application of uniaxial stress naturally leads to piezoelectric polarization regardless of the spin degree of freedom.

In the present study, we have investigated uniaxial-stress effects on magnetic and dielectric properties of a dysprosium orthoferrite $DyFeO_3$, which has a centrosymmetric crystal structure. This system is known to display a multiferroic nature in a magnetic-field-induced phase above ~3 T [18]. The multiferroicity can be described in terms of the magnetostriction between the magnetic moments on Fe and Dy atoms [18,19]. On the other hand, the ground state is an antiferromagnetic and nonferroelectric state. In this Letter, we report that an application of uniaxial stress induces ferroelectricity at the ground state. Moreover, the uniaxial-stress-induced ferroelectricity is accompanied by (weak) ferromagnetism. To the best of our knowledge, this is the first experimental observation of the "piezomagnetoelectric effect," namely, the simultaneous induction of both the electric polarization and ferromagnetic moment, in a single-phase compound. The present study also reveals that the induced ferromagnetic moment and electric polarization are tightly coupled with each other, indicating that the piezomagnetoelectric responses are of spin origin.

$DyFeO_3$ has an orthorhombically distorted perovskite structure, as shown in Fig. 1(b). In this Letter, we employed a conventional $Pbnm$ (orthorhombic) setting. The magnetic property of this system has been investigated since the 1960s [20,21]. At room temperature, the system exhibits the most conventional-type (G-type) antiferromagnetic order, in which the staggered Fe^{3+} spins direct nearly along the a axis, while the magnetic moments of Dy^{3+} ions are disordered. Because of the Dzyaloshinskii-Moriya (DM) interaction between the Fe spins, the spins are slightly canted from the a axis, yielding parasitic layered (A-type) antiferromagnetic and weak ferromagnetic components along the b and c axes, respectively [21]. According to Bertaut's notation [22], this magnetic

structure is described as $G_xA_yF_z$. We refer to this phase as the weak-ferromagnetic (WFM) phase.

With decreasing temperature in zero magnetic field, the system undergoes a magnetic phase transition from the WFM phase to an antiferromagnetic (AFM) phase around $T_{SR} = 40$ K. This transition was identified to be a reorientation of the majority G component from along the a axis to the b axis [20]. This spin reorientation leads to the disappearance of the WFM component, and instead, the canted spin components, namely the a and c components, exhibit the A-type and C-type orders, respectively. As a result, the magnetic order is described as $A_xG_yC_z$. This indicates that the direction of the G component is relevant to the weak ferromagnetism in this system.

With further decreasing temperature, Dy moments also exhibit an antiferromagnetic order below $T_N^{Dy} = 4$ K. We refer to this phase as the Dy-ordered AFM phase. According to a previous magnetization study on isostructural $DyAlO_3$ [23], the configuration of the Dy moments was reported to be G_xA_y. In Fig. 1(c), we show the spin arrangements in the Dy-ordered AFM phase. When a magnetic field is applied along the c axis in this phase, the system exhibits a magnetic-field-induced phase transition, at which the configuration of the Fe spins turns back to $G_xA_yF_z$, around $\mu_0H_{SR} \sim 3$ T. Tokunaga *et al.* have reported that the electric polarization appears along the c axis in the field-induced phase [18]. They explained the origin of the multiferroic nature by adapting the magnetostriction model to the nearest neighbor exchange coupling between the Fe spins and Dy moments, as shown in Fig. 1(c) [18,19].

Piezoelectric and piezomagnetic responses for these magnetic phases can be predicted in terms of the magnetic

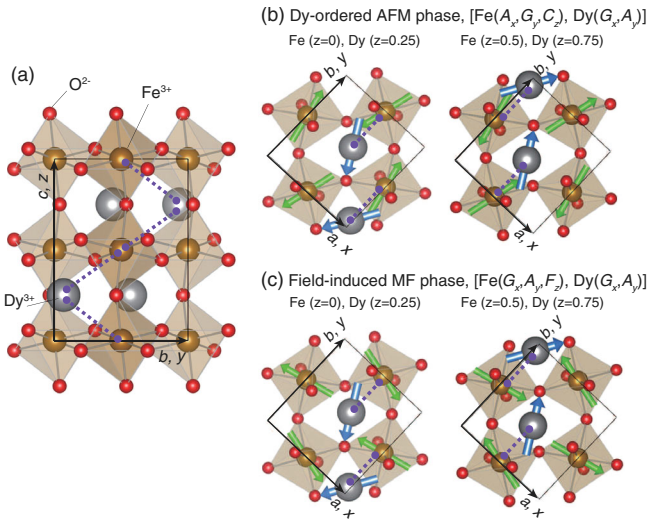

FIG. 1 (color online). (a) Crystal structure of $DyFeO_3$. Purple dotted lines show the paths of the nearest neighbor exchange coupling between the Fe spins and Dy moments. Magnetic structures of (b) the Dy-ordered AFM phase and (c) the field-induced multiferroic phase.

point group theory [20]. For example, the magnetic point group for the AFM phase and the Dy-ordered AFM phase are mmm and 222, respectively. By applying uniaxial stress along the (110) direction in the AFM phase, we can break two mirrors out of the three, and therefore the magnetic point group is reduced to $2/m$, which allows the ferromagnetic moment to appear along the c axis. Similarly, in the Dy-ordered AFM phase, an application of uniaxial stress along the (110) direction reduces the magnetic point group symmetry down to 2, leading to ferroelectric polarization as well as the ferromagnetic moment parallel to the c axis. To verify these symmetry arguments, we performed magnetization and pyroelectric measurements under applied uniaxial stress.

A single crystal of $DyFeO_3$ was grown by the floating-zone method and cut into a rectangular shape with the dimensions of $2.1 \times 2.3 \times 0.9$ mm^3. The widest surfaces were normal to the c axis, and two of the other surfaces were selected to be the (110) plane. The magnetization measurements were performed using the Magnetic Property Measurement System (Quantum Design Inc.) with the uniaxial-stress insert used in the previous studies [16,24]. For this experiment, we also developed a horizontal-uniaxial-stress cell, which is essentially the same as that used in the previous pyroelectric measurements on $Ba_2CoGe_2O_7$ [16]. The uniaxial compressive stress σ was applied on the (110) surfaces. Magnetic fields H were applied along the c axis. For the pyroelectric measurements, silver-paste electrodes were formed on the surfaces normal to the c axis in order to observe the electric polarization along the c axis (P_c). We also employed the uniaxial-stress insert for the Physical Property Measurement System, which was used in the previous studies [16,24,25]. We measured displacement electric current with varying temperature T or σ using an electrometer (Keithley 6517B). By integrating the current with respect to time, we deduced P_c. Note that the magnitudes of σ were calculated from the load applied from the top of the insert and the surface area of the sample in contact with the uniaxial-stress device.

Figure 2(a) shows the results of the magnetization measurements at 6 K in the AFM phase. We observed that the M-H curve shows a distinct hysteresis around $H = 0$ under σ, revealing that the application of σ induces weak ferromagnetism in the AFM phase. We also measured magnetization curves at 2 K under σ, as shown in Fig. 2(b). Although the changes in the M-H curve were rather small, we succeeded in observing the ferromagnetic hysteresis loops under σ by subtracting the data measured at $\sigma = 1$ MPa from the other data, as shown in Fig. 2(c). The remanent magnetization and coercive field increases and decreases with increasing σ, respectively. Note that the anomalies around ± 3 T are due to weak σ dependence of the critical field between the ground state and the field-induced phase.

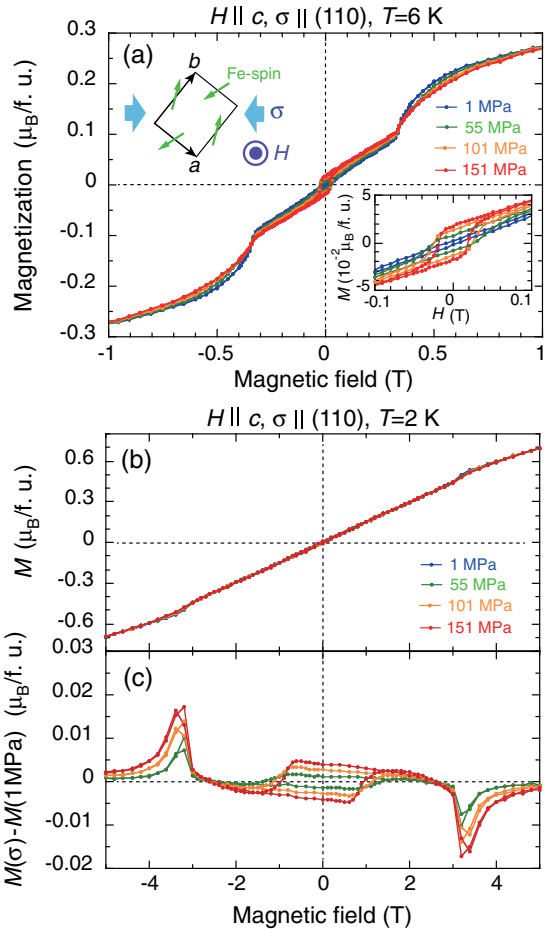

FIG. 2 (color online). (a) M-H curves observed at 6 K under applied σ of up to 151 MPa. The insets show (left, top) a schematic showing the directions of the Fe spins in the AFM phase, σ and H, and (right, bottom) a magnification of the hysteresis loops near $H = 0$. (b) M-H curves and (c) their differences from the data at $\sigma = 1$ MPa measured at 2 K under applied σ of up to 151 MPa.

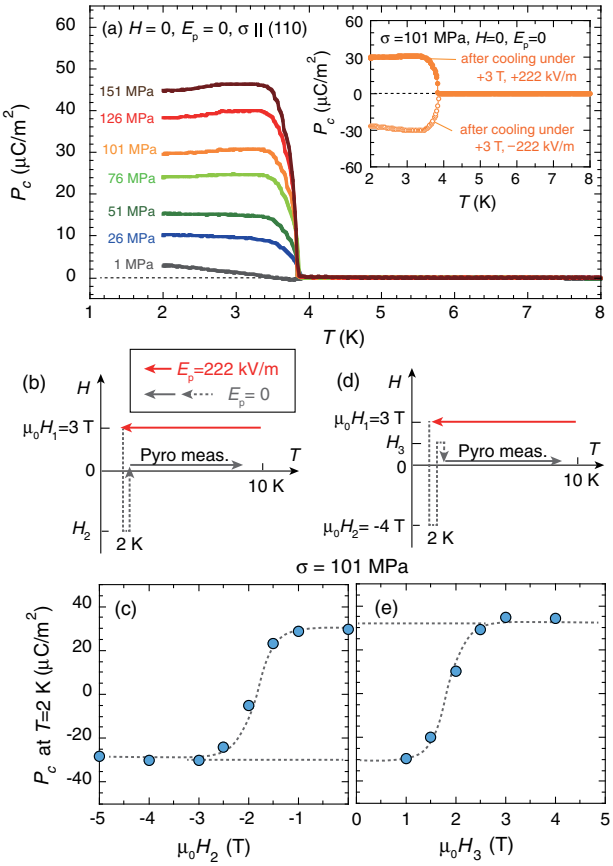

FIG. 3 (color online). (a) Temperature dependence of P_c measured on heating under applied σ without H and E_p. Before each measurement, the sample was cooled from 10 to 2 K under applied σ, $\mu_0 H = 3$ T, and $E_p = 222$ kV/m. The inset shows the data measured at $\sigma = 101$ MPa after cooling with positive and negative poling electric fields. (c) and (e) show the values of P_c at 2 K measured by pyroelectric measurements in zero magnetic field after temperature and magnetic field sequences shown in (b) and (d), respectively.

Figure 3(a) shows the results of pyroelectric measurements. Before these measurements, we applied σ, $\mu_0 H = 3$ T, and a poling electric field (E_p) of 222 kV/m at 10 K, and then cooled the sample down to 2 K. H and E_p were removed at 2 K. Subsequently, we measured pyroelectric current on heating under σ. We found that the application of σ induces spontaneous electric polarization along the c axis below T_N^{Dy}, and that the magnitude of P_c increases with increasing σ. We also observed that the sign of P_c was reversed when the sample was cooled in a negative E_p, as shown in the inset of Fig. 3(a). It is worth mentioning here that in the previous study on $Ba_2CoGe_2O_7$ [16], polarity of the piezoelectric polarization was determined only by direction of applied uniaxial stress. By contrast, in $DyFeO_3$, the application of σ induces a genuine "ferroelectric" state, in which the spontaneous electric polarization can be reversed by an application of electric field [26].

To confirm the that σ-induced ferroelectricity is of spin origin, we investigated H dependence of P_c as follows. We cooled the sample from 10 to 2 K under applied $\sigma = 101$ MPa, $\mu_0 H = 3$ T, and $E_p = 222$ kV/m. After removing E_p at 2 K, we changed the applied magnetic field from 3 T to a negative magnetic field of H_2, and then removed it, as shown in Fig. 3(b). Figure 3(c) shows H_2 dependence of the values of P_c at 2 K measured by pyroelectric measurements after the above mentioned sequences. We found that the σ-induced P_c was flipped by the application of $\mu_0 H_2$ below ~ -2 T. We also performed similar magnetic field sweeping sequences shown in Fig. 3(d), revealing that the flipped electric polarization was reversed again by applying a positive magnetic field of $\mu_0 H_3$ above ~2 T, as shown in Fig. 3(e). These results show that P_c exhibits the hysteresis loop with respect to the magnetic fields applied at 2 K. Moreover, the width of the hysteresis loop roughly agrees with that of the

M-H curves shown in Fig. 2(c). Although the agreement between these hysteresis loops is not perfect, this is probably because we measured the remanent electric polarization at $H = 0$ after sweeping the magnetic field up to a certain value, while we measured the magnetization with varying H. From these results, we concluded that P_c is coupled with the weak ferromagnetic moment, revealing that the σ-induced ferroelectricity originates from the spin order.

Figure 4(a) shows piezoelectric responses at 2 K in zero magnetic field. Before the measurements, the sample was cooled from 10 to 2 K under $\sigma = 101$ MPa, $\mu_0 H = 3$ T, and $E_p \pm 222$ kV/m. We removed H and E_p at 2 K, and then measured the displacement current with varying σ from 101 to 1 and then back to 101 MPa. The absolute values of P_c were determined by the subsequent pyroelectric measurements on heating. We observed that the σ-induced P_c changes in accordance with the varying σ, and that the polarity of the P_c changes depending on E_p applied on cooling.

Similarly, we also confirmed the piezomagnetic nature as shown in Fig. 4(b). We swept the magnetic field from 0 to 5 (or −5), and again to 0 T under σ at 2 K, and subsequently measured the spontaneous magnetization with varying σ from 101 to 1, and again to 101 MPa. We observed that the σ-induced ferromagnetic moment also shows a similar behavior to that of the σ-induced P_c. Note that the hystereses in these piezoelectric and piezomagnetic responses are probably due to the imperfect reduction of the stress; because of the friction between the zirconia pistons and anvils used in the pressure cell, the actual value of σ could not follow the nominal load value in particular in the σ-decreasing processes.

Here, we point out that the σ dependence of P_c in the σ-increasing process in Fig. 4(a) is in good agreement with

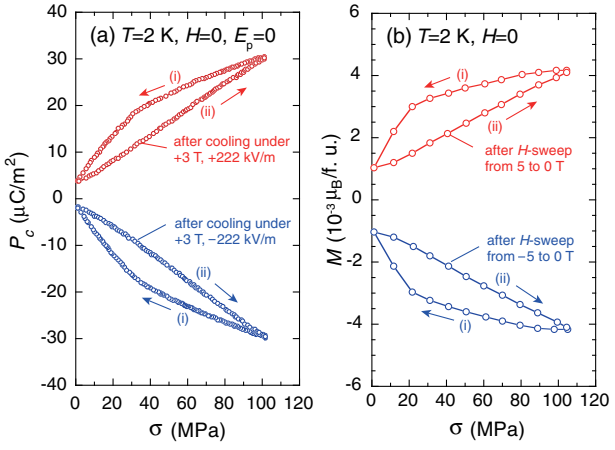

FIG. 4 (color online). (a) Piezoelectric responses measured at $T = 2$ K, $H = 0$, and $E_p = 0$ after cooling under $\sigma = 101$ MPa, $\mu_0 H = 3$ T, and $E_p \pm 222$ kV/m. (b) Piezomagnetic responses at $T = 2$ K in zero magnetic field measured after H sweeping from 0 to ±5 T and then to 0 T under $\sigma = 101$ MPa.

that obtained from the pyroelectric measurements shown in Fig. 3(a). Despite the differences in σ applied on cooling, we observed the same values of P_c at 2 K as a linear function of σ in both the measurements. These data are quite reproducible. These results exclude the possibility that the piezomagnetoelectric effect would be attributed to domain boundaries or coexisting minor metastable phase, which could appear depending on experimental conditions on cooling, and hence ensure that this effect is a bulk property and is well within a linear-response regime.

Finally, we discuss the microscopic picture of the uniaxial stress effects on the magnetic orders. As mentioned above, the disappearance of the weak ferromagnetism at T_{SR} is related to the rotation of the G component of Fe spins [20]. The present experiments demonstrate that an application of σ induces weak ferromagnetic moments in the AFM and Dy-ordered AFM phases. From these results, we suggest that the application of σ affects in-plane magnetic anisotropy of the Fe spins, so that they are slightly rotated from their original position. The rotation of the Fe spins can yield a small G_x component, which induces the spontaneous electric polarization in the Dy-ordered AFM phase via the magnetostriction mechanism, in the same manner as in the field-induced multiferroic phase [18,19]. By comparing the values of M and P_c in the Dy-ordered AFM phase under σ with those in the magnetic-field-induced multiferroic phase, the rotation angle is roughly estimated to be 1–2 degrees at $\sigma = 151$ MPa.

In summary, we have investigated uniaxial-stress effects on magnetic and dielectric properties of $DyFeO_3$, which has a centrosymmetric crystal structure. By means of magnetization and pyroelectric measurements, we revealed that an application of σ induces both the weak ferromagnetism and ferroelectricity in the Dy-ordered AFM phase. We also demonstrated that the magnetic-field-induced reversal of the weak ferromagnetic moment is accompanied by the flip of the electric polarization, revealing that the two σ-induced ferroic orders are coupled with each other. As for the microscopic mechanism of the uniaxial-stress effects, we suggest that the application of σ results in the change in magnetic anisotropy, which leads to a rotation of the Fe spins. This rotation yields the small G_x component of the Fe spins, which is relevant to the emergence of the weak ferromagnetism and also induces ferroelectricity through the magnetostriction mechanism. This work provides a new guiding principle for designing spin-driven multiferroicity. By applying anisotropic stress on an antiferromagnet, one can remove a number of symmetry operations in the system. This may lead to magnetically and electrically polarized states, in which the degree of the polarization can be tuned by the applied uniaxial stress. This guideline is also applicable for thin film samples [27–29], in which structural mismatch between the film and substrate often results in significant lattice deformation. It is worth mentioning that strain-induced multiferroicity has been

reported for epitaxial $EuTiO_3$ film [30], in which epitaxial strain is isotropic in lateral directions and strongly affects frequency of a polar phonon mode [31]. By contrast, the present study suggests that an antiferromagnetic film on a substrate with in-plane anisotropy may possibly exhibit non-IDM type spin-driven multiferroicity, which arises from a combination of symmetries of magnetic order and underlying chemical lattice deformed by epitaxial strain.

This work was supported by Grants-in-Aid for Young Scientists (A) (No. 25707032) and (B) (No. 25800203) from JSPS, Japan. The images of the crystal and magnetic structures in this Letter were depicted using the software VESTA [32] developed by K. Momma.

*taro.nakajima@riken.jp

[1] T. Kimura, T. Goto, H. Shintani, K. Ishizaka, T. Arima, and Y. Tokura, Nature (London) **426**, 55 (2003).
[2] M. Fiebig, J. Phys. D **38**, R123 (2005).
[3] T. Arima, J. Phys. Soc. Jpn. **80**, 052001 (2011).
[4] Y. Tokura, S. Seki, and N. Nagaosa, Rep. Prog. Phys. **77**, 076501 (2014).
[5] T. Kimura, G. Lawes, T. Goto, Y. Tokura, and A. P. Ramirez, Phys. Rev. B **71**, 224425 (2005).
[6] M. Kenzelmann, A. B. Harris, S. Jonas, C. Broholm, J. Schefer, S. B. Kim, C. L. Zhang, S.-W. Cheong, O. P. Vajk, and J. W. Lynn, Phys. Rev. Lett. **95**, 087206 (2005).
[7] G. Lawes, A. B. Harris, T. Kimura, N. Rogado, R. J. Cava, A. Aharony, O. Entin-Wohlman, T. Yildrim, M. Kenzelmann, C. Broholm *et al.*, Phys. Rev. Lett. **95**, 087205 (2005).
[8] K. Taniguchi, N. Abe, T. Takenobu, Y. Iwasa, and T. Arima, Phys. Rev. Lett. **97**, 097203 (2006).
[9] I. A. Sergienko and E. Dagotto, Phys. Rev. B **73**, 094434 (2006).
[10] H. Katsura, N. Nagaosa, and A. V. Balatsky, Phys. Rev. Lett. **95**, 057205 (2005).
[11] M. Mostovoy, Phys. Rev. Lett. **96**, 067601 (2006).
[12] C. Jia, S. Onoda, N. Nagaosa, and J. H. Han, Phys. Rev. B **76**, 144424 (2007).
[13] T. Arima, J. Phys. Soc. Jpn. **76**, 073702 (2007).
[14] I. A. Sergienko, C. Şen, and E. Dagotto, Phys. Rev. Lett. **97**, 227204 (2006).
[15] S. Picozzi, K. Yamauchi, B. Sanyal, I. A. Sergienko, and E. Dagotto, Phys. Rev. Lett. **99**, 227201 (2007).
[16] T. Nakajima, Y. Tokunaga, V. Kocsis, Y. Taguchi, Y. Tokura, and T.-h. Arima, Phys. Rev. Lett. **114**, 067201 (2015).
[17] H. Murakawa, Y. Onose, S. Miyahara, N. Furukawa, and Y. Tokura, Phys. Rev. Lett. **105**, 137202 (2010).
[18] Y. Tokunaga, S. Iguchi, T. Arima, and Y. Tokura, Phys. Rev. Lett. **101**, 097205 (2008).
[19] Y. Tokunaga, Y. Taguchi, T.-h. Arima, and Y. Tokura, Nat. Phys. **8**, 838 (2012).
[20] G. Gorodetski, B. Sharon, and S. Shtrikman, J. Appl. Phys. **39**, 1371 (1968).
[21] G. Gorodetsky and D. Treves, Phys. Rev. **135**, A97 (1964).
[22] E. F. Bertaut, *Magnetism* (Academic Press, New York, 1963), Vol. 3.
[23] L. M. Holmes, L. G. Van Uitert, R. R. Hecker, and G. W. Hull, Phys. Rev. B **5**, 138 (1972).
[24] T. Nakajima, S. Mitsuda, K. Takahashi, K. Yoshitomi, K. Masuda, C. Kaneko, Y. Honma, S. Kobayashi, H. Kitazawa, M. Kosaka *et al.*, J. Phys. Soc. Jpn. **81**, 094710 (2012).
[25] T. Nakajima, S. Mitsuda, T. Nakamura, H. Ishii, T. Haku, Y. Honma, M. Kosaka, N. Aso, and Y. Uwatoko, Phys. Rev. B **83**, 220101 (2011).
[26] The original definition of ferroelectricity is that electric polarization can be reversed by an application of electric field in an isothermal condition. However, we could not achieve the isothermal reversal of P_c, because the maximum electric field in the present experimental setup (200–300 kV/m) was smaller than coercive electric field, that is typically 1–3 MV/m in the field-induced multiferroic phase of $DyFeO_3$ [18].
[27] T.-Y. Khim, M. J. Eom, J. S. Kim, B.-G. Park, J.-Y. Kim, and J.-H. Park, Appl. Phys. Lett. **99**, 072501 (2011).
[28] M. Nakamura, Y. Tokunaga, M. Kawasaki, and Y. Tokura, Appl. Phys. Lett. **98**, 082902 (2011).
[29] J. Wang, J. B. Neaton, H. Zheng, V. Nagarajan, S. B. Ogale, B. Liu, D. Viehland, V. Vaithyanathan, D. G. Schlom, U. V. Waghmare *et al.*, Science **299**, 1719 (2003).
[30] J. H. Lee, L. Fang, E. Vlahos, X. Ke, Y. W. Jung, L. F. Kourkoutis, J.-W. Kim, P. J. Ryan, T. Heeg, M. Roeckerath *et al.*, Nature (London) **466**, 954 (2010).
[31] C. J. Fennie and K. M. Rabe, Phys. Rev. Lett. **97**, 267602 (2006).
[32] K. Momma and F. Izumi, J. Appl. Crystallogr. **41**, 653 (2008).